

Many-Body Line Shape in X-Ray Photoemission from Metals

G. K. Wertheim and S. Hüfner*

Bell Laboratories, Murray Hill, New Jersey 07974

(Received 16 April 1975)

It is shown that Mahan-Nozières-De Dominicis singularity provides a highly accurate description of the shape of x-ray-photoemission lines in metals. This strongly suggests that this mechanism must have general validity in core-level spectroscopies.

Although the relevance of the Mahan-Nozières-De Dominicis¹⁻³ (MND) many-body phenomenon to the interpretation of core-level photoemission spectra has been long recognized, no attempt has so far been made to test this theory in detail, e.g., by a direct comparison of experimental and theoretical line shapes. We report here the results of an analysis of core-electron line shapes obtained by x-ray-photoemission spectroscopy (XPS), taking into account both the instrumental resolution function and the many-body line shape. The results obtained provide strong support for the validity of the many-body formalism, and in addition shed some light on the question of its range of validity, and on the magnitude and form of the inelastic component in XPS data.

In this comparison we use the line-shape function of Doniach and Sunjic,⁴

$$I(\epsilon) = \frac{\cos[\pi\alpha/2 + (1-\alpha)\arctan \epsilon/\gamma]}{(\epsilon^2 + \gamma^2)^{(1-\alpha)/2}}, \quad (1)$$

in which ϵ is the energy measured from the threshold of the unbroadened line, γ is the lifetime width, and α is an asymmetry parameter defined by

$$\alpha = 2 \sum_{l=0}^{l_{\max}} (2l+1)(\delta_l/\pi)^2, \quad (2)$$

where the δ_l are the partial-wave phase shifts. One can readily verify that the above equation reduces to a Lorentzian when $\alpha = 0$, and approaches $1/\epsilon^{(1-\alpha)}$, i.e., the form of the MND singularity, when $\epsilon/\gamma \ll -1$. (For $\epsilon/\gamma \gg 1$ the equation retains an essentially Lorentzian character.) As we have previously pointed out,⁵ attempts to compare this equation directly with photoemission data are frustrated by instrumental broadening which is comparable to the lifetime width of many core levels in instruments currently available. Deconvolution to remove the instrumental contribution is at best an imperfect solution because in all practical cases some of the instrumental width will remain.⁵ The alternative approach is

to convolve the theoretical line shape with the instrumental resolution function. This is in many respects the more desirable approach because it leaves the data in their natural state, and puts less exacting requirements on our knowledge of the resolution function.⁶

We have determined the resolution function for a HP 5950A spectrometer from measurements on the Fermi edge of silver and from very narrow core lines in nonmetals. If we assume that the Fermi edge is not itself subject to many-body distortions, then its derivative gives the instrumental resolution function, provided kT is small compared to instrumental contributions. These analyses show that the resolution function is itself slightly skewed, but does not have a long tail. It may be represented over a limited range by the two-parameter form

$$G(\epsilon) \propto \exp\{-[a\epsilon/(1+\beta\epsilon)]^2\}, \quad (3)$$

where β is a skewness parameter which typically has a value of 0.12–0.14, and a is 3.0 eV⁻¹.

Data for this study were taken on a number of metals, surface cleaned in the spectrometer vacuum by mechanically removing a macroscopic surface layer with a tungsten carbide blade. This technique generally provides a cleaner surface than obtained by vacuum evaporation because it avoids the pressure rise associated with the heating of the furnace. Sputter-deposited or sputter-cleaned surfaces were avoided in the knowledge that such surfaces often have properties quite different from those of the metal itself.⁷ Oxygen and carbon contamination were negligible in the data used here.

The results obtained by this process are illustrated in Fig. 1. Note first of all that the data (represented by the points) have not been modified or corrected in any way; no background subtraction has been done, no smoothing, and no deconvolution. The theoretical line shape (represented by the solid line) is determined by two parameters, γ and α . In practice γ is deter-

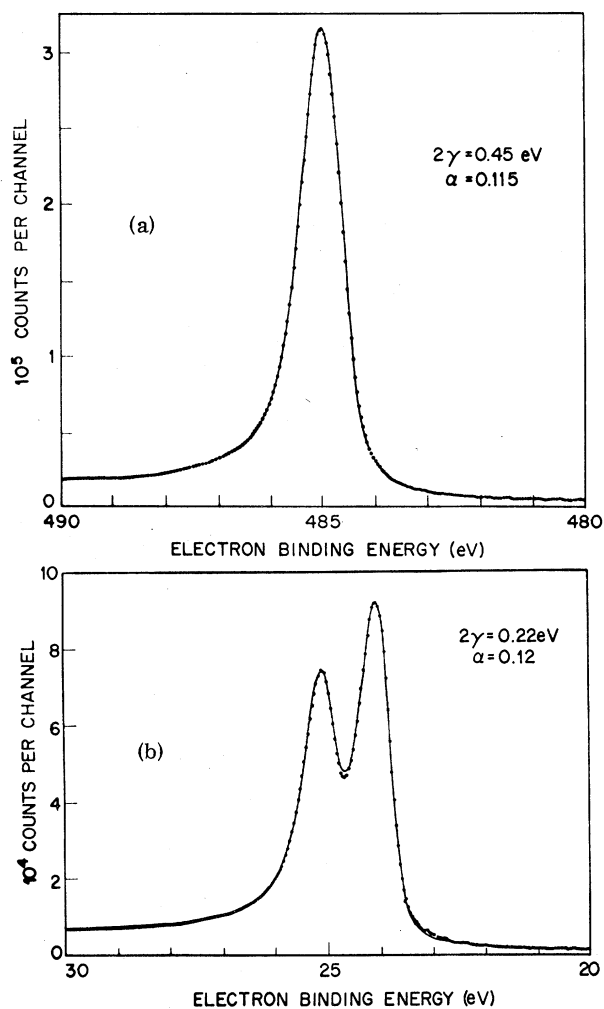


FIG. 1 (a) X-ray photoemission spectrum of the tin $3d_{5/2}$ core level fitted by Eq. (1) as described in the text. The data are represented by the points, the equation by the line. The plasmon is sufficiently far removed that it does not affect the background. (b) The $4d_{3/2}$ and $4d_{5/2}$ levels of tin, treated as in (a).

mined by the shape of the right-hand part of the line, and α by the shape of the left-hand part. Two other parameters, which determine the height and position, are essentially trivial since they do not influence the shape. The same is true of a *constant* background which is entirely determined by the level at the right-hand end of the spectrum. The instrumental resolution function is treated as a known constant. The uncertainty in α is ± 0.01 .

A single fit of this quality could easily be dismissed as an accident due to a fortuitous cancellation of various distortions in the spectrum. This skepticism becomes harder to maintain

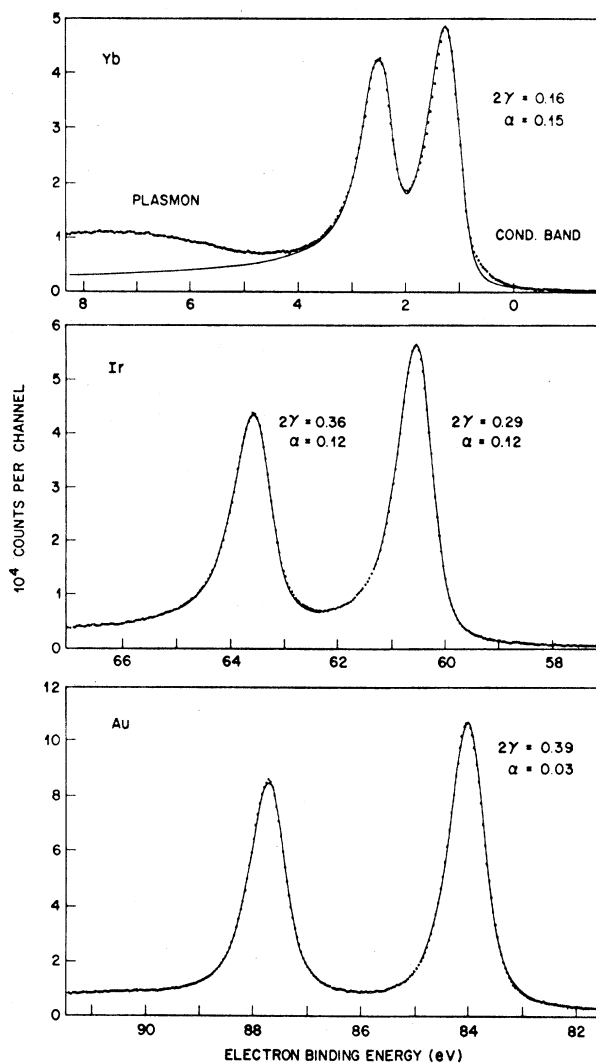


FIG. 2. The $4f$ levels of Yb, Ir, and Au, treated as in Fig. 1. The theoretical 3:4 spin-orbit intensity ratio was used. Although close to the Fermi energy, the Yb levels show little if any band-structure characteristics. The fit to the Ir data from Ref. 5 is much more satisfactory than that obtained after deconvolution. In the case of Au a small linear background was added to take into account the effects of plasmons evident on a wider scan.

when it is found that other lines in the same metal are fitted equally well, changing only one parameter, the lifetime width; see Fig. 1(b). The intensities of the two spin-orbit components were given their theoretical 2:3 ratio. Results of similar quality have been obtained for a wide variety of metals; see Fig. 2. More detailed results will be published elsewhere.⁸

The good agreement between theoretical and ex-

perimental line shapes has a number of implications. The derivation of the MND singularity is such that its validity is assured only in the immediate vicinity of the singularity. The range of validity and the nature of the cutoff have not been established. The present data suggest that for $0.05 \leq \alpha \leq 0.25$ the equation remains a good approximation over at least 5 eV from the singularity itself. At greater distances the problem becomes obscured by the plasmon which inevitably accompanies the photoemission line. This leads to the second point which concerns the energy-loss tail which is said to accompany XPS lines. It is often assumed that this tail may be represented as a step function starting at, and accompanying, each δ -function line element. The present results give no indication that such a tail is present; only the well-known plasmon is found. This in turn suggests that background subtraction may be an ill-conceived process designed to symmetrize an inherently asymmetric line. This would also explain why attempts to fit XPS lines with the Voigt function after background subtraction are seldom wholly satisfactory. It should be recognized, however, that the area of the plasmon peak is proportional to the area of the parent line. Wide lines will therefore have more prominent plasmons, and may well overlap the plasmon peak itself. Under these circumstances a line may appear to be superposed on a rising background, but it is still incorrect to assume that the background at any point is proportional to the integral of the spectrum taken toward smaller binding energy.

Considering the small escape depth, 15 Å, from which unscattered photoelectrons are collected, it is surprising that no structure attributable to the surface layer of atoms is resolved in these experiments. Electron binding energies of surface atoms apparently do not differ by more than a few tenths of an eV from those of bulk atoms in the cases studied. The only exceptions are Pd and Pt where additional unexplained structure was reported in Ref. 5.

In the course of this work a large number of metals have been investigated. The examples presented in this paper were selected to show the generality of the phenomena in different kinds of metals: s - p band metals (Sn), f -band metals (Yb), d -band metals with d density of states at the Fermi energy (Ir), and noble metals with quite small d -band density of states at the Fermi energy (Au). For a quantitative interpretation we assume that for all these metals an analysis

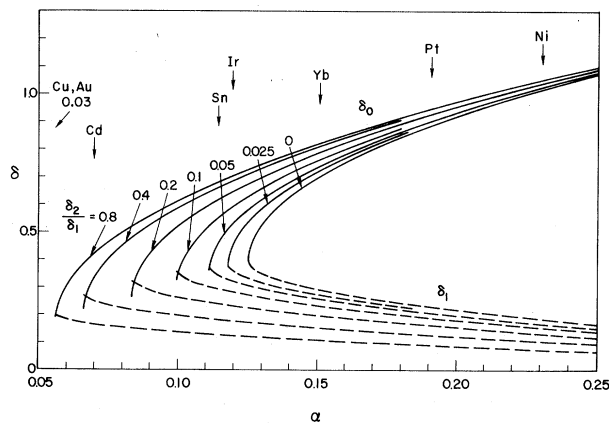


FIG. 3. Phase shifts δ_0 and δ_1 as a function of α in a three-phase-shift analysis.

in terms of s , p , and d phase shifts is required. (Even in Yb, because of the narrowness of the f band and the corresponding small density of states at the Fermi energy, this should be a good approximation.) The Friedel sum rule provides one constraint, leaving one free parameter. Interpretation will be based on Fig. 3 which shows δ_0 and δ_1 as functions of α with δ_2/δ_1 taken as the parameter.

Figure 3 shows that for Sn, where δ_2 is presumably small, δ_0 and δ_1 will be 0.45 ± 0.10 and 0.30 ± 0.05 , respectively. In Ir and Yb, where the d density of states is sizable (δ_2 large), δ_0 is quite well determined and respectively of the order of 0.7 and 0.8. The large δ_0 in these materials is probably a result of the s - d resonance mechanism for the enhancement of the δ_0 contribution suggested by Kotani and Toyozawa.⁹ Finally, the small α values for the noble metals, like Au, require s , p , d , and f contributions with appreciable δ_2 phase shifts in agreement with the admixture of d character in their conduction bands.

In the only other determination of asymmetry parameters from XPS spectra, Ley *et al.*⁶ used only two points on single lines of Mg, Al, and Li and thus did not test the validity of the theory. Their results are at variance with those obtained following the procedures outlined here.¹⁰ Their analysis determined only one phase shift which, at least for Al and Mg, is inappropriate.

In summary, the lines observed in XPS experiments on metals have for the first time been shown to be accurately described by a line-shape function derived from the MND many-body theory. The "customary" background subtraction

was not required, and it is argued that in view of the present results this background correction must be viewed with suspicion. The parameters governing the many-body singularities derived in this way are the most accurate available to date. A quantitative interpretation of these parameters is in most cases only possible within limits because of the complexity of the band structures. Finally, in view of these results, it is hard to escape the conclusion that the MND theory must also apply in other spectroscopies which involve the generation of core holes in metals.¹¹

*Permanent address: Fachbereich Physik, Freie Universität, Berlin, Republic of West Germany.

¹G. D. Mahan, Phys. Rev. **163**, 612 (1967).

²P. Nozières and C. T. De Dominicis, Phys. Rev. **178**, 1097 (1969).

³See also K. D. Schotte and U. Schotte, Phys. Rev.

182, 479 (1969); D. C. Langreth, Phys. Rev. **182**, 973 (1969).

⁴S. Doniach and M. Sunjic, J. Phys. C: Proc. Phys. Soc., London **3**, 285 (1970).

⁵S. Hüfner and G. K. Wertheim, Phys. Rev. B **11**, 678 (1975).

⁶Other recent work has not attempted a comparison between theoretical and experimental line shapes. See, for example, S. Hüfner, G. K. Wertheim, D. N. E. Buchanan, and K. W. West, Phys. Lett. **A46**, 420 (1974); N. J. Shevchik, Phys. Rev. Lett. **33**, 1336 (1974); L. Ley, F. R. McFeely, S. P. Kowalczyk, J. G. Jenkin, and D. A. Shirley, Phys. Rev. B **11**, 600 (1975).

⁷S. Hüfner, G. K. Wertheim, and D. N. E. Buchanan, Chem. Phys. Lett. **24**, 527 (1974).

⁸S. Hüfner, G. K. Wertheim, and J. H. Wernick, to be published.

⁹A. Kotani and Y. Toyozawa, J. Phys. Soc., Jpn. **35**, 1082 1073 (1973), and **37**, 912 (1974).

¹⁰G. K. Wertheim and P. H. Citrin, unpublished.

¹¹See J. D. Dow, Phys. Rev. B **9**, 4165 (1974), for a summary of attempts to demonstrate the MND mechanism in other spectroscopies.

Chemical Bonding and Structure of Metal-Semiconductor Interfaces

J. M. Andrews

Bell Laboratories, Allentown, Pennsylvania 18103

and

J. C. Phillips

Bell Laboratories, Murray Hill, New Jersey 07974

(Received 9 April 1975)

New results and new microscopic models are presented to describe chemical trends in barrier heights at transition-metal-silicide-silicon interfaces and at nontransition-metal-silicon interfaces, where in the latter case a very thin oxide is present.

Broadly speaking there are four kinds of interfaces between metals and nonmetals. Each type is characterized by specific interfacial atomic configurations and chemical interactions. Within each type the barrier height ϕ_B for thermionic emission of electrons across the interface exhibits characteristic chemical trends.¹⁻³ The four types are as follows: (1) The nonmetal is an insulator, and the metal is physisorbed on the insulator surface. (2) The nonmetal is a highly polarizable ($\epsilon > 7$)³ semiconductor (such as Si) and the metal does not react with it to form a bulk compound (weak chemical bonding). (3) The nonmetal is a highly polarizable semiconductor and there are one or more bulk compounds which can be formed between it and the metal (strong

chemical bonding). (4) The surface preparation (e.g., by chemical etching rather than by cleaving in very high vacuum) of the highly polarizable semiconductor has left a very thin oxide between it and the metal (bonding mediated by a native dielectric).

Type (1) is a true Schottky barrier, in which ϕ_B is nearly proportional to ϕ_m , the metal work function.⁴ Type (2) is a Bardeen barrier,⁵ in which ϕ_B is nearly independent of ϕ_m . In this Letter we propose for the first time microscopic models of the potentials associated with interfaces of types (3) and (4). These models account for the chemical trends in ϕ_B observed for types (3) and (4). The chemical trend of type-(3) interfaces as reported here is new, while the trend